Microencapsulation of Intumescent Flame-Retardant Agent: Application to Flame-Retardant Natural Rubber Composite

Jincheng Wang, Yuehui Chen

College of Chemistry and Chemical Engineering, Shanghai University of Engineering Science, Shanghai 201620, China

Received 25 February 2006; accepted 18 July 2006
DOI 10.1002/app.25835
Published online in Wiley InterScience (www.interscience.wiley.com).

ABSTRACT: The first part of this investigation focused on the synthesis and characterization of a microencapsulated intumescent flame retardant (MIFR) agent. Two steps were used in the synthesis process. The structure was characterized by scanning electron microscopy, thermogravimetric anaylysis, and Fourier transform infrared spectroscopy. The addition of this MIFR agent into natural rubber (NR) led to an improvement in its physicomechanical and flame-retardant (FR) properties. The second part focused on the evaluation of such characteristics as cure characteristics, FR property, tensile properties, abrasion resistance, and dynamic mechanical analysis of MIFR filled NR composites. © 2007 Wiley Periodicals, Inc. J Appl Polym Sci 104: 1828–1838, 2007

Key words: flame retardance; microencapsulation; characterization; natural rubber

INTRODUCTION

Natural rubber (NR) is a material that has shown its worthiness both as a ''commodity polymer'' and as an ''engineering elastomer'' by virtue of its unique combination of physicomechanical properties. NR has some unique advantages over competitive synthetic rubbers such as properties required for special applications like manufacture of aerotires, suspension elements, various latex products, etc. Despite a number of superior qualities, one of the setbacks of NR that limits its usage for highly demanding applications such as coal mine conveyor belts, power cables, aircraft tire treads, etc., is its inherently high flammability.[1,2]

One way to decrease the flammability of polymer materials is chemical modification by using phosphorus-containing reagents or monomers. The advantage of this method is the inclusion of active species in the polymer structure, and they cannot diffuse toward the polymeric material surface and remain more efficient longer. Another way is to introduce a flame-retardant (FR) additive. The use of intumescent additives allows both fire properties and mechanical behavior of the materials to be optimized.[3–6] An intumescent flame-retardant (IFR) system usually contains three main substances: an acid source, a carbon source, and a gas source. They are usually used in combinations and the typical example is the composite of ammonium-polyphosphate (APP), pentaerythritol (PER), and melamine (ME).[7] During the heating process, an IFR agent generates a cellular charred layer on the surface of the material, which protects the underlying material from the action of the heat flux or flame, and act as a physical barrier that limits the diffusion of combustible volatile products toward the flame, and of oxygen toward the polymer. The proposed mechanisms are based on the charred layer acting as a physical barrier, which slows down heat and mass transfer between the gas and condensed phases.[8,9]

However, intumescent formulations with IFR agents are unfortunately not permanent. Indeed, these agents are water-soluble, and they have a poor compatibility with the polymeric materials. Thus, problems of migration and solubility may occur. The microencapsulation of IFR agents could avoid these problems. Microencapsulation is a process of enveloping microscopic amounts of matter in a thin film of polymer, which forms a solid wall.[10,11] This shell/core structure allows isolation of the encapsulated substance from the surroundings, and thus protects it from any degrading factors such as water. The encapsulated substance can be liberated by fusion or dissolution of the impermeable shell or by diffusion across a porous shell.[12,13]

It is of interest to study microencapsulation of the IFR agents with a melamine-formaldehyde (MF)

Correspondence to: J. Wang (wjc406@263.net).

Contract grant sponsor: Shanghai Leading Academic Discipline Project; contract grant number: p1402.
Contract grant sponsor: Shanghai Educational Commission Foundation; contract grant number: 06NZ006.

shell for two main reasons. First, we can expect that the microcapsules with this shell will be compatible with the NR polymer matrix. Second, combination of the encapsulated IFR agent with MF shell could be an efficient FR intumescent formulation, which could be introduced into NR systems to protect them.

In the present work, we initially describe the preparation of IFR agent coated by MF resin by a two-step method. Then, the capsulated shells and the related properties of the MIFR agent are characterized by scanning electron microscopy (SEM), thermogravimetric anaylysis (TGA), and Fourier transform infrared (FTIR) spectroscopy. However, the main interest in this work is to study the physical and mechanical properties of the MIFR filled NR composites including cure characteristics, flame retardance, tensile strength, abrasion resistance, and dynamic mechanical analysis (DMA).

EXPERIMENTAL

Materials

To prepare this new MIFR agent, APP ($(NH_4PO_3)n$, $H = 700$, Hostamflam 422, Hoechest, soluble fraction in H_2O: < 1 wt %), PER (Aldrich), and ME (Aldrich) were supplied by Shanghai Organic Plant, and were all used as received; methanol, formaldehyde, and triethanolamine (analytical pure) were provided by Yixing Zhoutie Jieli Chemical Plant.

To compare the FR, physical and mechanical properties between IFR/NR and MIFR/NR composites, following formulation, which was presented in Table I, is used.

Preparation of MIFR agent

The following two-step method was used to prepare the MIFR agents. The first step was to prepare oligomer of MF resin. Eighty grams of formaldehyde solution with a mass concentration of 36%, 7 g of methanol and 24 g of triethanolamine were put into a three-necked flask. Then, the reaction mixture was heated to 85°C and kept for 2 h. Twenty-one grams of ME was added to the heated mixture and the new mixture was heated to 90°C. After the suspension became transparent, it was kept for 6 h at the same temperature and the solution was then cooled to room temperature in air. The oligomer of MF was ready for the next step.

The second step was to prepare MIFR agents. The above MF oligomer was added into a three-necked flask containing 28 g of IFR agent (APP : PER : ME = 3 : 1 : 1, wt %) and 73 mL of distilled water. The pH of the mixture was adjusted to 4.5–5.0 with aqueous hydrochoric acid. The mixture was stirred for 0.5 h and heated to 100°C for 1 h. Then, the reaction mixture was left to cool to room temperature. The product was filtered, washed three times with distilled water, and dried to constant weight at 80°C. The white MIFR powders were then obtained.

A schematic illustration of preparation procedure of MIFR by a two-step polymerization process is shown in Scheme 1.

TABLE I
Formulation of NR Vulcanizates

Ingredients	Loading (phr)
NR	100
Sulfur	2.5
Zinc oxide	5.0
Stearic acid	1.0
2-benzothiazolethiol	1.2
Tetramethyl thiuram disulfide	0.2
Diphenyl guanidine	0.3
Electric insulating oil	8.0
IFR or MIFR	0/40/50/60/70/80

Preparation of IFR/NR and MIFR/NR composites

IFR/NR and MIFR/NR composites were prepared on a double roller plasticator, operating at 20°C. The sheeted compounds were conditioned at 20°C for 24 h before testing.

The curing parameters were determined on an o cillating disk rheometer (TI-100, Technologia Industrial) according to ASTM D 2084-81. The compositions were then vulcanized at 150°C during the optimum cure times under 15 MPa pressure on an electrically heated press. To compare the test results conveniently, all of the uncured mixes and vulcanizates in this article were prepared using the above conditions and the formulation shown in Table I except for the change of the amount of IFR or MIFR agent.

Characterization of MIFR agent and MIFR/NR composites

FTIR spectroscopy

FTIR spectra were recorded on a Nicolet 170SX FTIR spectrophotometer (Nicolet Analytical Instruments, Madison, WI) in the range 4000–600 cm^{-1} at a resolution of 2 cm^{-1}. Samples were ground and mixed with KBr to form pellets. Sixty-four scans were necessary to obtain spectra with good signal-to-noise ratios.

Photography and scanning electron microscopy

Scanning photographs of the horizontal burning test were taken by a digital Sony camera. SEM analysis of the MIFR agent and the typical fracture surface of

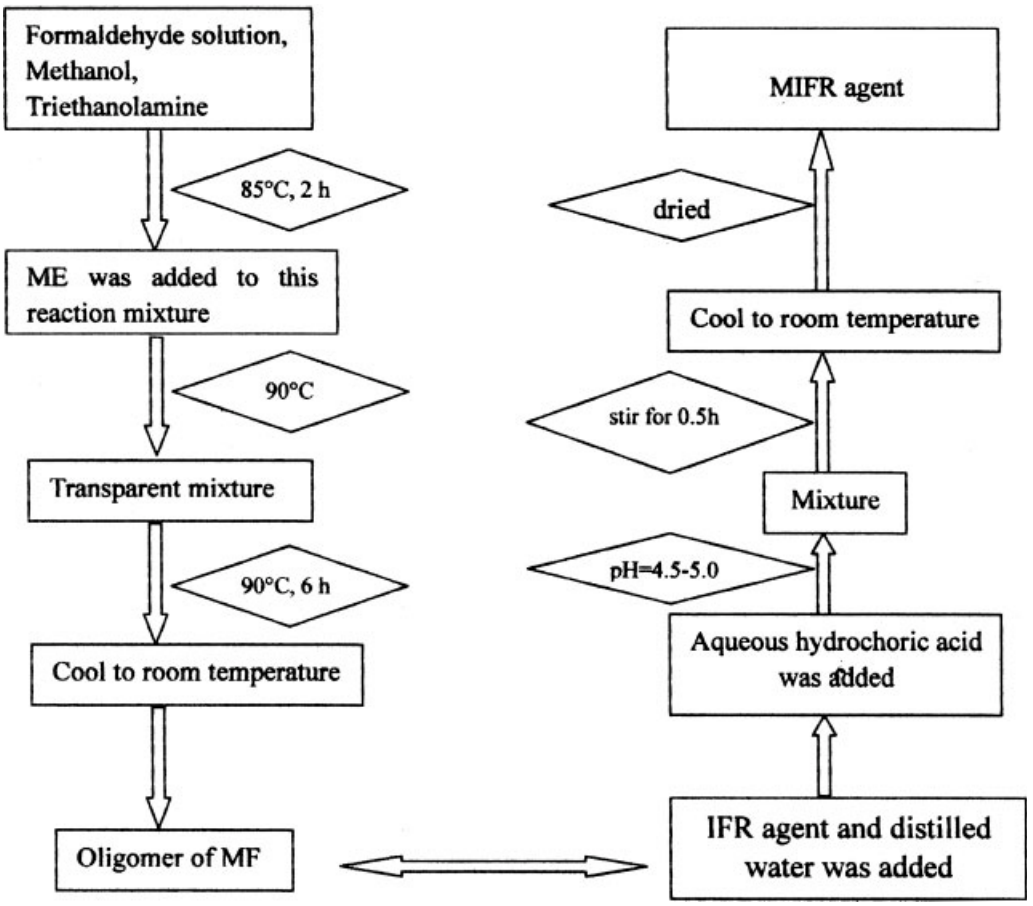

Scheme 1 Preparation procedure of MIFR agent by a two-step polymerization process.

different NR composites was carried out using Comscan Series 4 instrument. The samples were gold coated using an IB-3 Ionic sputtermeter.

FR tests

Limiting Oxygen Index (LOI) was measured using a Stanton Redcroft instrument on sheets ($100 \times 10 \times 3$ mm^3) according to ASTM 2863.

Samples ($100 \times 100 \times 10$ mm^3) were exposed to a Stanton Redcroft cone calorimeter according to ASTM 1356-90 under a heat flux of 50 kW/m^2 (this external flux has been chosen because it corresponds to the heat evolved during a well-developed fire). Three tests have been practiced on each material and average results were extracted from these tests that limits the uncertainties on the measurements.

The flame retardance of NR composites was also evaluated by UL-94 test according to ASTM D-635-77.

Thermal analysis

Thermogravimetric analysis (TGA) was carried out at 10°C/min under air (flow rate 5×10^{-7} m^3/s, air liquid grade) using a DuPont 1090 microbalance. In each case, the mass of samples used was fixed at 10 mg and the samples (powder mixtures) were positioned in open vitreous silica pans. The precision of the temperature measurements was 1°C over the whole range of temperatures.

Mechanical properties

The tensile properties of the vulcanizates were measured with dumbbell specimens (6 mm wide in cross section) according to the Chinese National Standard GB 528-82. The value for each sample was taken as the median value of five specimens. These tests were carried out at room temperature on an Instron universal testing machine, with a crosshead speed of 500 mm/min. The tensile specimens for each composition were tested and the stress and strain at break determined. Hardness measurements were performed according to GB 531-83 on a Shore A hardness tester.

The dynamic mechanical properties were measured using a Rheometric Scientific DMA analyzer (Model MK III; Polymer Laboratories, Poole, UK) under the following conditions: frequency, 1 Hz;

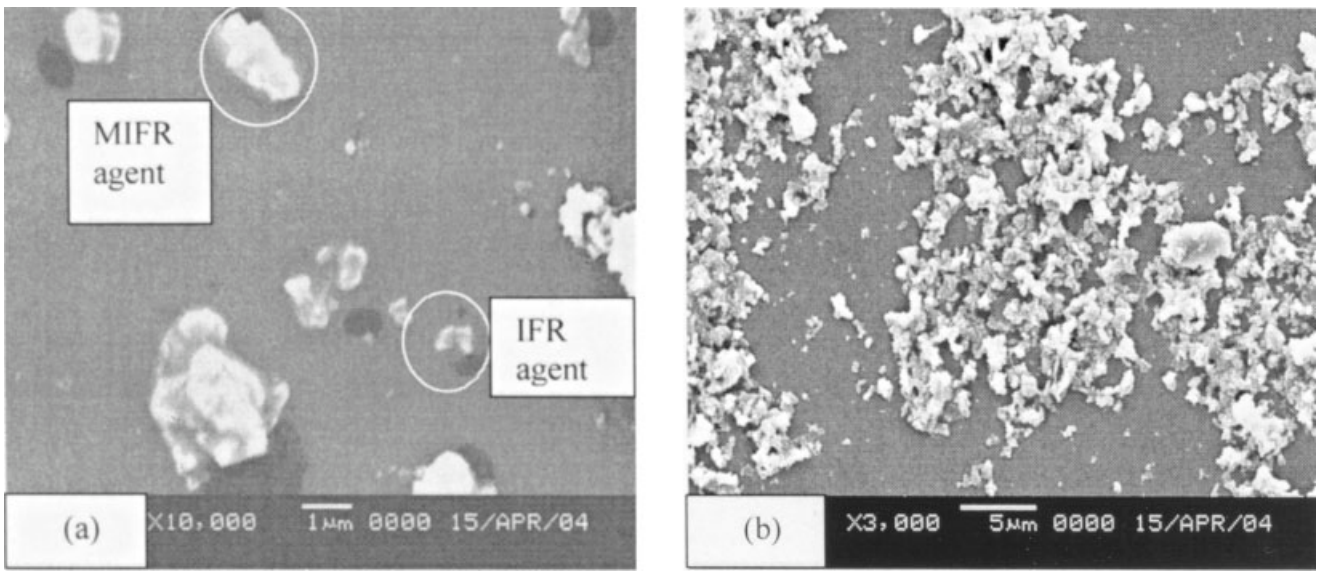

Figure 1 SEM pictures of MIFR agent at different magnifications (a) ×10,000; (b) ×3000.

heating rate, 2°C/min; single-cantilever bending mode, and temperature ranging from −100 to 10°C.

RESULTS AND DISCUSSION

Characterization of the MIFR agent

SEM analysis

Figure 1 presents SEM images of the MIFR agent at different magnifications. It is clear that the MIFR agent is bigger and the surface is rougher than that of the IFR agent, because it is coated by a polymer layer.[14] From the pictures, it can also be seen that the diameter of the IFR agent is about 0.1–0.5 μm and the MIFR agent is about 2 μm, and the core of this microcapsule may contain more than one IFR powder.

Thermal analysis

TGA curves of the MF oligomer, microcapsule shell, IFR, and MIFR agents are presented in Figure 2. The MIFR agent has an enhanced thermal behavior in comparison with that of the IFR agent. MF oligomer is a linear polymer and the thermal stability of which is much poor, and almost three degradation steps can be seen from Figure 2(a). This oligomer first shows initial weight loss at 110°C, and the second step of which is observed between 200 and 350°C. The last step occurs at 350°C, and 5 wt % residue is remained when temperature arises higher than 700°C. Figure 2(b) shows TGA study under air of microcapsule shell we synthesized, and it demonstrates that the thermal stability of the MF oligomer is greatly improved after crosslinking reaction. Its degradation under air occurs in two successive steps. The first step starts at about 200°C and lasts till 440°C. At higher temperature, the degradation continues, and leaves a residue about 10 wt %. With regard to the degradation of the IFR agent, which is shown in Figure 2(c), it also contains three steps. Between 180 and 250°C, the first step occurs. The second step occurs at 250°C followed by the formation of a carbonaceous material relatively stable in the temperature range 450–500°C, and finally a stable residue about 20 wt % left. Figure 2(d) shows TGA of the MIFR agent, and it presents almost two reaction steps during thermal degradation. First, a pyrolysis occurs between 200 and 500°C. Then, the intumescent material develops followed by the formation of a carbonaceous material relatively stable

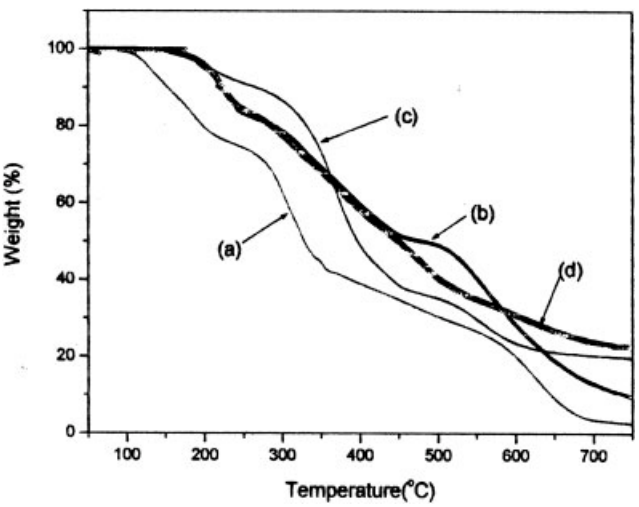

Figure 2 TGA curves of (a) MF oligomer; (b) microcapsule shell; (c) IFR agent; (d) MIFR agent.

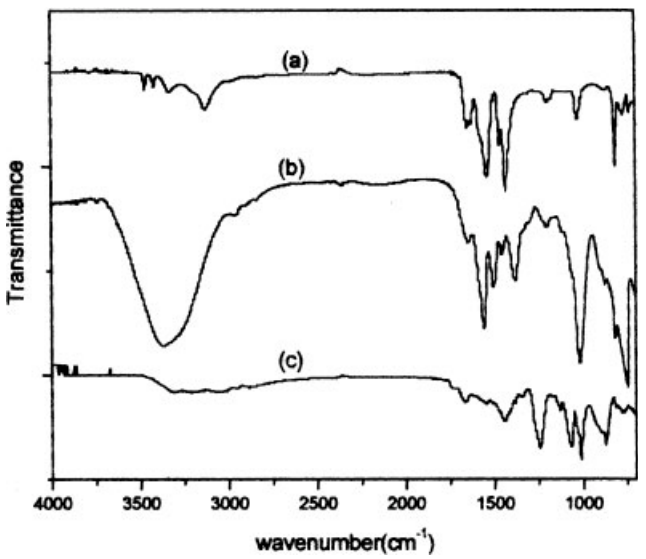

Figure 3 FTIR spectra of (a) ME; (b) MF oligomer; (c) microcapsule shell.

in the temperature range higher than 500°C, and finally, the degradation of this material occurs successively with a stable residue about 25 wt %.[15]

FTIR analysis

Figure 3(a–c) show the FTIR spectra of ME, MF oligomer, and the final microcapsule shell, respectively. It is observed from Figure 3(a), the ME spectrum, that there are two obvious absorption peaks at 1500 and 810 cm^{-1}, which correspond to the in-plane and out-of-plane bending vibrations of the aromatic structure in the triazine group. The characteristic absorptions at 3400 and 1680 cm^{-1} result from the stretching and bending vibrations of $—NH_2$ presented in the raw material. In the spectrum of the MF oligomer as shown in Figure 3(b), the main absorption peaks appear at 3350, 2920, 1575, 1060, and 810 cm^{-1}. The obvious absorption peak of 3350 cm^{-1} was because of the —NH and —OH stretching vibration in MF oligomer. The absorption peaks at 1575, 1060, and 810 cm^{-1} were ascribed to the ring vibration of triazine group. The absorption peak at 2920 cm^{-1} was attributed to C—H stretching vibration of alkyl groups, which were connected to the triazine rings. As shown in Figure 3(c), FTIR spectrum of the microcapsule shell, the characteristic absorptions at 3300 cm^{-1} result from the stretching vibrations of —NH group. The increased stretching absorptions at 1060 and 1260 cm^{-1} are related to the increased amount of C—O—C group, due to the crosslinking reaction between the oligomer molecular chains. The obvious decrease of absorption peak at 3300 cm^{-1} illustrates the amount decease of —OH in the microcapsules shell, which may be caused by thorough chemical reactions such as condensation polymerization between —OH groups.[16]

General remarks

Regarding SEM, TGA, and FTIR analysis results, we may conclude that the microcapsule shell formation may conform to the following process as shown in Scheme 2, and the corresponding chemical equations are illustrated in Scheme 3. Scheme 3(a,b) show the formation of linear MF oligomer, and triethanolamine used in this reaction may supply the alkalescent environment for the process of this reaction. Scheme 3(c) depicts the possible formation of the crosslinked microcapsules shell by condensation polymerization of MF oligomer, and the aqueous hydrochoric acid used in this reaction is to catalyze the formation of the microcapsule shells.

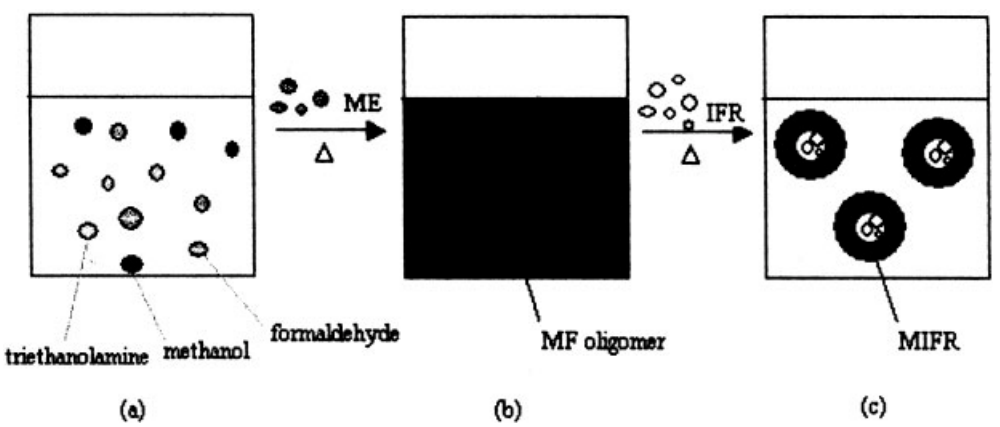

Scheme 2 MIFR formation process (a) raw materials; (b) MF oligomer; (c) MIFR agent.

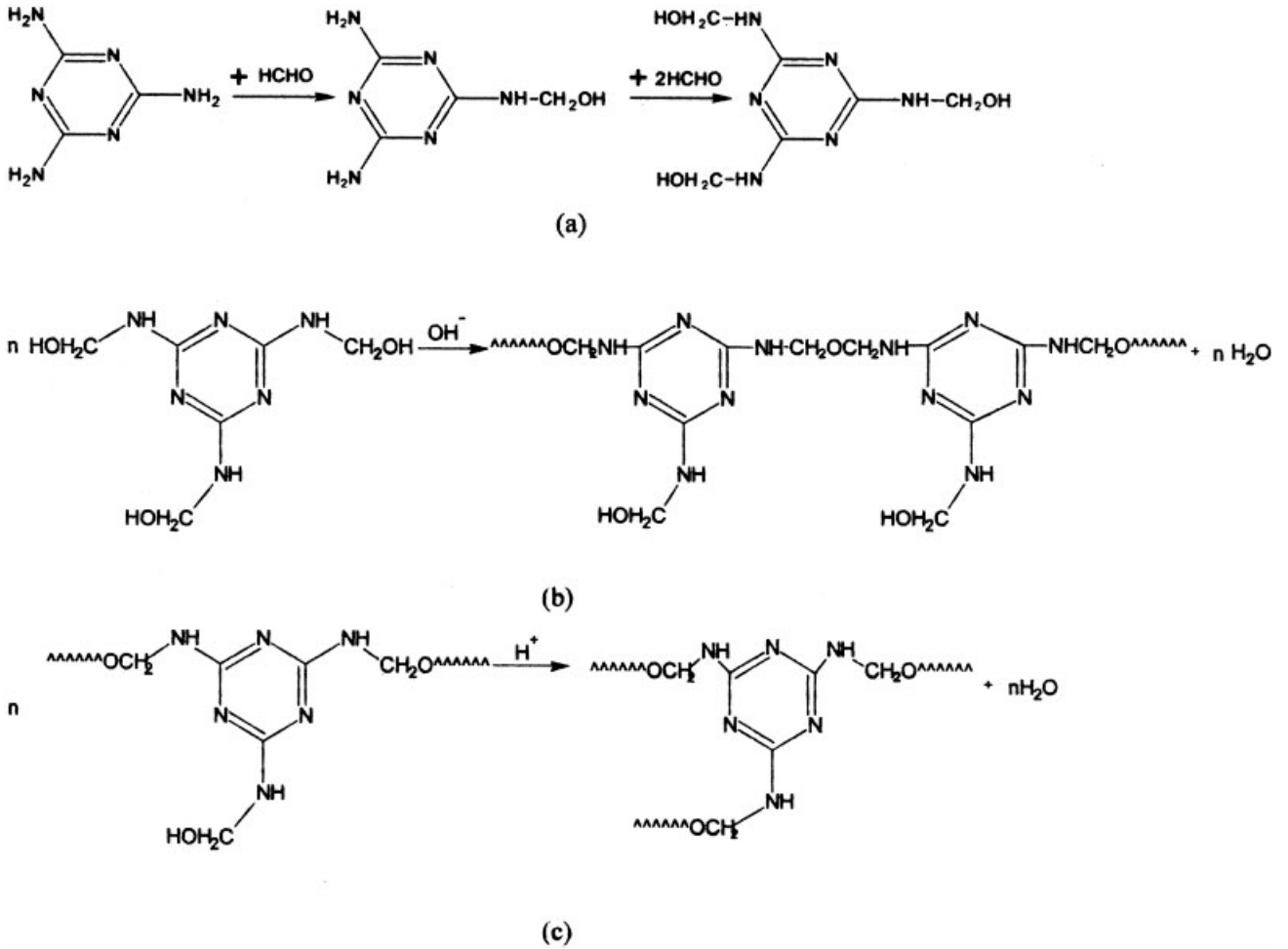

Scheme 3 Microcapsule shell formation reaction that was assumed to occur.

Characterization of the MIFR/NR composites

Cure characteristics

The data for the cure characteristics of the IFR/NR and MIFR/NR composites are summarized in Table II.

Compared with the IFR/NR composites, it can be seen that the addition of the MIFR agent (40–70 phr) can prolong scorch time (t_{10}) and make processing safer; also, it can be concluded that a retardation effect occurs in the vulcanization process deduced from the prolonged technical cure time (t_{90}). Meanwhile, the increase of initial and minimum torque (M_0 and M_L), which shows an increase of viscosity, can make MIFR/NR system not easier to process. This phenomenon may result from the ''plastic effect'' of the MF shell on the MIFR/NR composites. The maximum torque (M_m) can be taken as a measurement of crosslinking density. From the results we can see that the crosslinking density of MIFR/NR increases with the amount increase of the MIFR agent, and the composite of IFR/NR shows the opposite phenomenon. This can illustrate that the microcapsule shell of the MIFR agent can increase the interfacial interaction between the IFR agent and the NR matrix, and thus increase the crosslinking density of the composite.[17]

Fire retarding performance

The evaluation of fire retarding performance shows that the formulation containing the MIFR agents has better performance than the formulation with the same amounts of the IFR agent.

TABLE II
Cure Characteristic of the Different NR Systems[a]

Formulation	Loading (phr)	t_{10}	t_{90}	M_0	M_L	M_m
IFR/NR	40	0.95	3.85	0.123	0.111	1.613
	50	0.98	4.02	0.135	0.128	1.562
	60	1.02	4.26	0.141	0.137	1.396
	70	1.08	5.64	0.152	0.149	1.168
MIFR/NR	40	1.02	4.15	0.142	0.154	1.585
	50	1.08	4.68	0.150	0.163	1.633
	60	1.14	5.90	0.161	0.175	1.789
	70	1.20	7.70	0.181	0.189	1.901

[a] t_{10}, scorch time (min); t_{90}, technical cure time (min); M_0, initial torque (lb.in.); M_L, minimum torque (lb.in.); M_m, maximum torque (lb.in.).

TABLE III
LOI Value and UL-94 Ratings of NR, IFR/NR, and MIFR/NR Systems

Loading (%)	IFR/NR		MIFR/NR	
	LOI (%)	UL-94 rating	LOI (%)	UL-94 rating
0	16.0	V_2	16.0	V_2
40	21.5	V_1	22.5	V_1
50	23.0	V_1	24.5	V_1
60	24.5	V_1	26.5	V_1
70	26.0	V_1	27.5	V_0

The LOI and UL-94 ratings of NR, IFR/NR, and MIFR/NR systems are listed in Table III. The LOI value of pure NR is very low (16.0), which means that NR is easily flammable.[18] By adding 40–70 phr IFR agent into pure NR, the LOI value increases to 26.0. With the addition of 40–70 phr MIFR into system, the LOI value increases to 27.5, and shows better fire protection for NR (UL-94 V-0, 70 phr), which means that the MIFR agent can delay the pyrolysis process of the blends, and improve the FR properties for the NR system. This is probably because of the synergistic effect of flame retardance between the shell (MF resin) and the core (IFR agent). The photos, which are shown in Figure 4, are the images of horizontal burning tests after extinguishment of fire for the NR composites incorporated with 70 phr IFR and 70 phr MIFR agents. From Figure 4(a,b), we can see that the char layer of MIFR-70/NR composite is relatively thicker compared with that of the IFR-70/NR system, which may be caused by the intumescent effect of MF shell on the system.

Thermal analysis

TGA study under air of the IFR-70/NR and MIFR-70/NR systems is shown in Figure 5. Figure 5(a), the formulation of a carbonaceous material under air in the IFR-70/NR composite occurs in three successive steps. The first step, with a peak at about 350°C, may be assigned to the reaction between the IFR agent and the NR system. Then, the development of intumescent material occurs followed by the formation of a carbonaceous material relatively stable in the temperature range 450–600°C, and finally a stable residue about 18 wt % left.

In the case of formulation with the MIFR agent as shown in Figure 5(b), it presents almost the same reaction steps during thermal degradation. First, a first degradation occurs between 300 and 450°C. Then, a carbonaceous material develops and degrades in the temperature range 450–550°C, and finally, a stable residue about 22 wt % is remained when temperature arises higher than 550°C.

FR performance

All parameters of dynamic flammability of the IFR-70/NR and MIFR-70/NR systems tested by cone calorimeter are listed in Table IV.

From Table IV, we can see that the MIFR-70/NR system has lower THR, RHR, EHC values, compared with that of the IFR-70/NR system, which indicates that the MIFR-70/NR system has less fire hazard.

TTI is an important index that can be used to evaluate the FR property of the polymeric materials. The bigger the value, the more effective the material.[19]

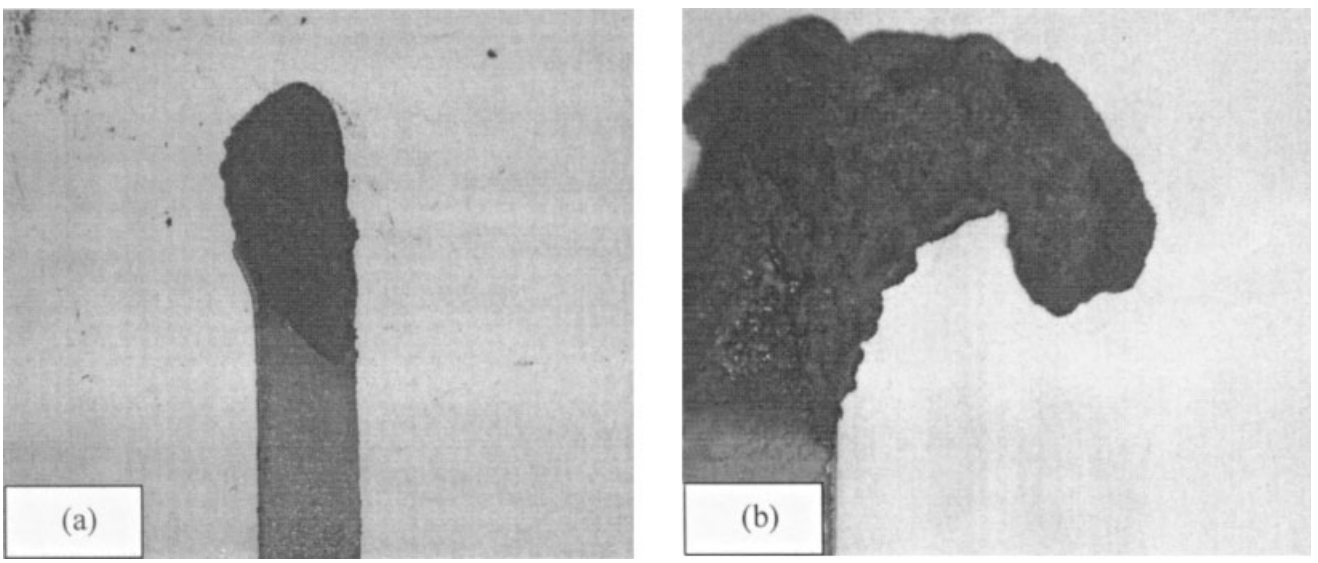

Figure 4 Char layer photos of (a) IFR-70/NR; (b) MIFR-70/NR.

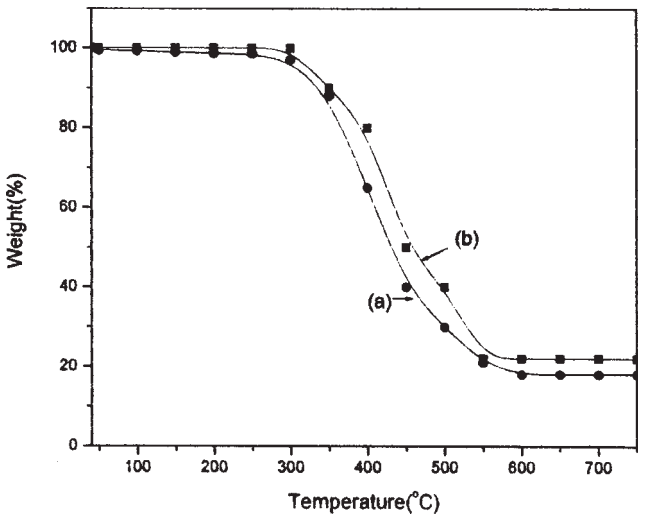

Figure 5 TGA curves of (a) IFR-70/NR (b) MIFR-70/NR systems under air.

From Table IV, we can see that the addition of the MIFR agent in the NR system makes the TTI shorter, which indicates the early flammability of the system. This result can also be seen from other intumescent systems.[19–21] This phenomenon is due to the acceleration of thermal degradation and rapid surface char formation. Also, it can be seen from Table IV that the presence of the MIFR agent reduces RHR in comparison with that of the IFR agent. The MIFR-70/NR system also has a significantly lower EHC. It is because, while burning, a foamed multi-cellular char on the surface of the material makes a thermal insulation and provokes the extinguishment of the flame, and this can also be seen from Figure 4. The char layer prevents combustion gases from feeding the flame, separates oxygen from feeding the flame and also separates oxygen from the burning material. The toxicity of smoke during combustion is a parameter that can also be evaluated by cone calorimeter test. It is evident that, during combustion, the MIFR-70/NR has higher SEA, CO and CO_2 concentration than that of the IFR-70/NR. This may be ascribed to the degradation of MF shell during combustion. This result clearly illustrates the MF shell may increase the incomplete combustion of the NR composite.

TABLE IV
Comparison of Dynamic Flammability Between IFR-70/NR and MIFR-70/NR Composites

	IFR-70/NR	MIFR-70/NR
Initial mass (g)	90.0	90.0
Mass loss (%)	74.0	70.0
Time to ignition (s)	20	18
Total heat released (THR) (kJ)	1669.7	1539.6
Rate of heat release (RHR) (kW/m^2)		
Maximum	789.2	689.3
Average	515.9	486.9
Effective heat of combustion (EHC) (MJ/kg)		
Maximum	28.0	25.9
Average	24.9	21.6
Specific extinction area (SEA) (m^2/kg)		
Maximum	994.9	1089.2
Average	499.5	525.3
Carbon monoxide (CO) evolution (kg/kg)		
Maximum	0.069	0.079
Average	0.058	0.068
Carbon dioxide (CO_2) evolution (kg/kg)		
Maximum	3.998	4.154
Average	1.688	2.249

Mechanical properties

Tensile properties

The results given in Table V show that the MIFR-70/NR composite becomes softer with the addition of the MIFR agent. Compared with the IFR-70/NR system, the improvement in tensile strength, elongation at break, and abrasion resistance is expected because of the improving compatibility between the MIFR agent and the NR matrix.[22] This can also be confirmed from SEM images of its fracture surface which is shown in Figure 6. As what can be seen from Figure 6(a), some voids, which were caused by the IFR agents, can be clearly seen from the fracture surface, and thus led to the decreasing tensile properties of the system. As for the MIFR incorporated system, shown in Figure 6(b), voids are rarely seen in the polymer matrix and better compatibility can be seen in this system, and that is the reason why this composite shows better tensile properties. Figure 7 shows the photos of worn surfaces of the IFR and MIFR agents filled systems, respectively. It can be seen that the worn surface of the MIFR filled system accumulated stacks of rubber scraps, while the composite containing the IFR agents appears a relatively flat surface. A phenomenon can be seen during the abrasion test is that a lot of powder fell during the abrasion test of the IFR-70/NR system, and that is why the worn surface of this system is relatively flat. The reason for the rubber scraps appearing in the worn surface of the MIFR-70/NR composite may be caused by the higher compatibil-

TABLE V
Tensile Properties of Different NR Systems

	Properties			
Formulation	Tensile strength (MPa)	Elongation at break (%)	Hardness (SHA)	Abrasion loss (cm^3)
NR	8.20	427	48.7	0.2546
IFR-70/NR	7.66	480	62.2	0.4747
MIFR-70/NR	8.26	696	35.6	0.3966

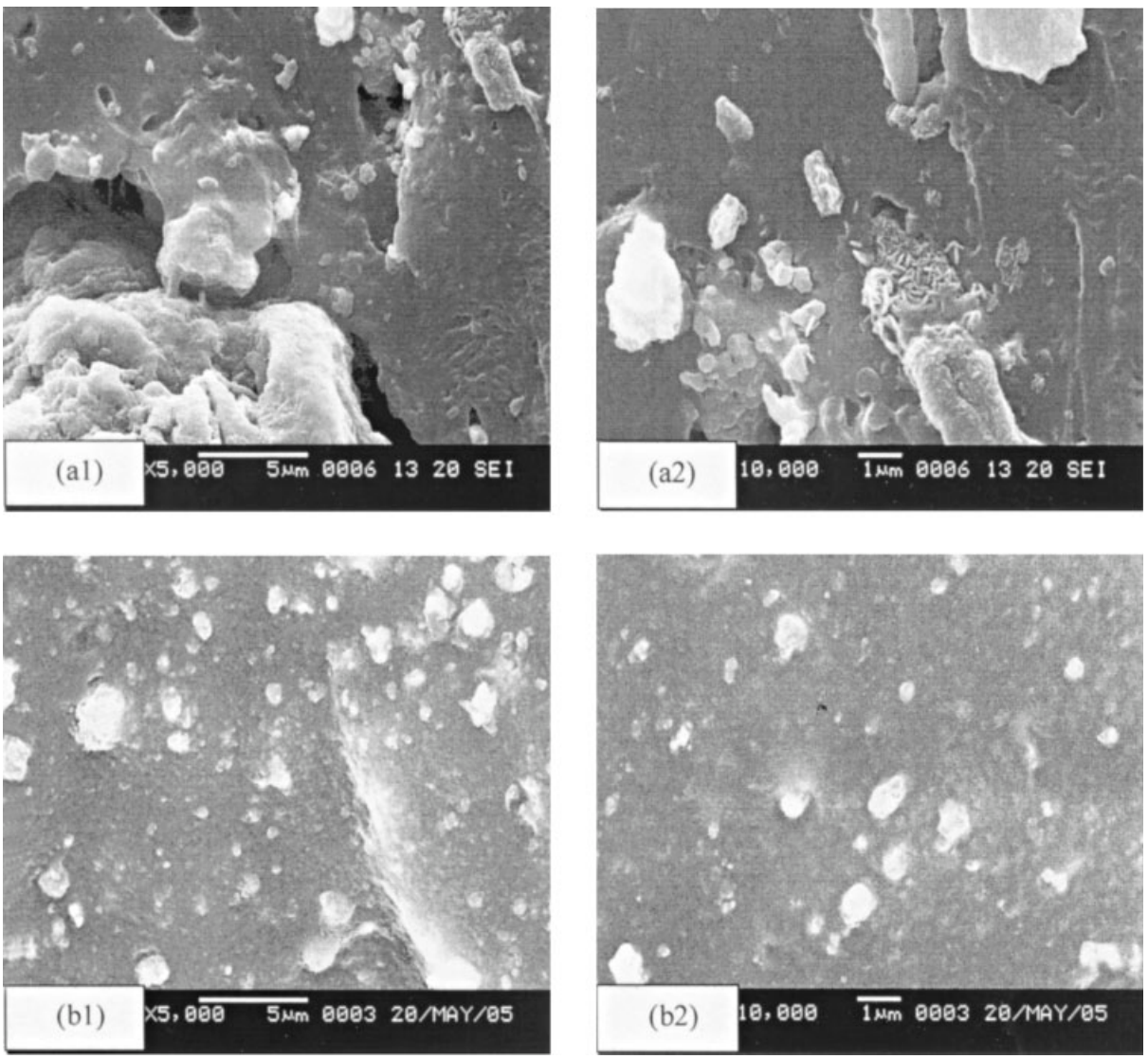

Figure 6 SEM images of (a-1,2) IFR-70/NR; (b-1,2) MIFR-70/NR systems.

ity of the MIFR fillers with the NR matrix, which leads to higher crosslinking level and not easily worn out for this system.

DMA analysis

Dynamic mechanical properties were measured to examine the degree of filler-matrix interaction in the NR composites. Figure 8 shows the effect of incorporation of 70 phr IFR and MIFR agent on the storage moduli and loss tangent of the NR composites as a function of temperature. Figure 8(a) shows the variation of storage modulus (E′) with temperature. Before glass transition, the storage modulus of the IFR-70/NR composite lies relatively higher compared to the MIFR-70/NR system. This indicates that there is higher interfacial action between the rubber matrix and the IFR fillers in the IFR/NR composite. Having in mind that the working tempera-

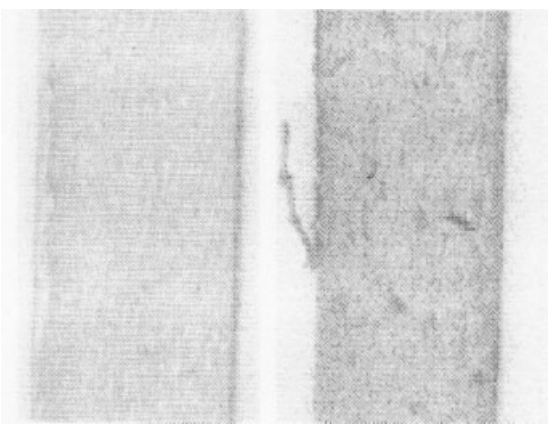

Figure 7 Photos of worn surfaces (a) IFR-70/NR; (b) MIFR-70/NR systems.

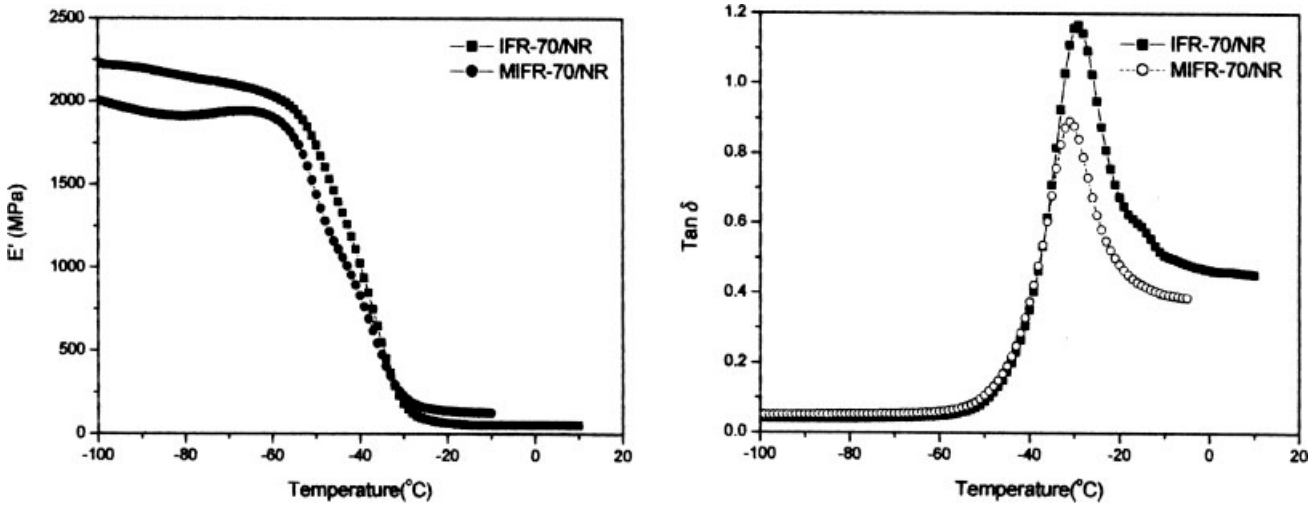

Figure 8 DMA curves of different NR systems (a) storage modulus versus temperature; (b) loss tangent versus temperature.

ture of rubber is usually above their glass transition (T_g), the plateau values of the E′ in this region is of great importance. Examination of E′ bending modulus above T_g reveals that addition of the MIFR agent can slightly improve the bending modulus of the system, and this is probably due to the better compatibility and higher crosslinking level in this composite. This result is in good accordance with the tensile properties of the two NR composites. Figure 8(b) shows the variation of loss curves (tan δ) with temperature. An intense peak at −29 and −30°C appears respectively, in the main storage modulus drop of the two NR systems. This suggests that this peak is associated with the main glass transition of the two composites. It can be seen that the glass transition temperature was slight decreased with the addition of the MIFR agent, which illustrates that the easier mobilization of the NR polymer chains influenced by the incorporating MF shells. The obvious decrease of intensity of tan δ may be attributed to the decrease of friction force between polymer chains and the MIFR fillers, which illustrates that the MF shell can act as a plasticizer in the composites.[23,24]

CONCLUSIONS

A type of microencapsulated IFR agent with MF shells was synthesized and was used as FR agent for NR systems. The expected advantages of this new concept of encapsulated FR agent lie in its being compatible with the NR polymeric matrix to give an efficient FR and mechanical properties.

Microcapsules and their components (e.g., IFR agent and MF shell) have been examined by TGA in air and FTIR analysis. The physicomechanical properties of NR composites loaded with different amounts of IFR and MIFR agents were studied and compared. It was demonstrated that the NR composite filled with 70 phr MIFR agent shows better FR, tensile and abrasion properties compared to the IFR-70/NR system.

Further work will be needed to improve the cure and dynamic flammability properties such as SEA, CO, and CO_2 concentration of the MIFR/NR composite, and the evaluation of FR mechanism of this composite is also needed.

References

1. Derouet, D.; Radhakrishnan, N.; Brosse, J. C.; Boccaccio, G. J Appl Polym Sci 1994, 52, 1309.
2. Menon, A. R. R. J Fire Sci 1997, 15, 3.
3. Wang, J. C.; Yang, S. L.; Li, G.; Jiang, J. M. J Fire Sci 2003, 21, 245.
4. Wang, J. C.; Li, G.; Yang, S. L.; Jiang, J. M. J Appl Polym Sci 2004, 91, 1193.
5. Le Bras, M.; Bugajny, M.; Lefebvre. J Polym Int 2000, 49, 1115.
6. Bourbigot, S.; Le Bras, M.; Bugajny, M. Intumescence and Polymer Blending: An Approach for Flame Retardancy, NIST Annual Conference, Gaithersburg, 1998.
7. Camino, G.; Costa, L.; Trossarelli, L. Polym Degrad Stab 1984, 6, 243.
8. Bourbigot, S.; Le Bras, M.; Delobel, R. J Chem Soc Faraday Trans 1996, 92, 149.
9. Mamleev, V. Sh.; Gibov, K. M. In Fire Retardancy of Polymers: The Use of Intumescence; The Royal Chem Society: Cambridge, 1998.
10. Giraud, S.; Bourbigot, S.; Rochery, M.; Vroman, I.; Tighzert, L.; Delobel, R. Polym Degrad Stab 2002, 77, 285.
11. Thie, C. Encyclopedia of Polymer Science and Engineering, Microencapsulation, 2nd ed.; Wiley: New York, 1987.
12. Jansen, L. J. J. M.; te Nijenhuis, K. J Membr Sci 1992, 65, 59.
13. Jansen, L. J. J. M.; te Nijenhuis, K.; Boersma, A. J Membr Sci 1993, 79, 11.
14. Qiang, W.; Jiangping, L.; Baojun, Q. Polym Int 2003, 52, 1326.
15. Wang, J. C.; Chen, Y. H. J Fire Sci 2005, 23, 55.

16. Lan, X. Z.; Tan, Z. C.; Zhou, G. L.; Sun, L. X.; Zhang, T. Chin J Chem 2004, 22, 411.
17. Wang, J. C.; Chen, Y. H.; Wang, J. H. J Elast Plast 2005, 37, 169.
18. Zheng, F. Properties and Design Application of Rubber Materials; Chem Industry: Beijing, 2003.
19. Ding, W. Doctoral Dissertation, Beijing University of Science and Technology, 2001.
20. Pagliari, A.; Cicchetti, O.; Bevilacqua, A. Flame Retardants'92'; The Plastics and Rubber Institute: London, 1992.
21. Marchal, A.; Delobel, R.; Le Bras, M. Polym Degrad Stab 1994, 44, 263.
22. Woycheshin, C. A.; Sobolev, I. In Handbook of Fillers and Reinforcements for Plastics; Van Nostrand Reinhold: New York, 1978.
23. Pramanik, M.; Srivastava, S. K.; Samantaray, B. K. J Appl Polym Sci 2003, 87, 2216.
24. Konstantinos, G. G.; Nikolaos, S. S.; Anton, A. Macromol Mater Eng 2004, 289, 1079.